Transp Porous Med (2008) 73:141–159
DOI 10.1007/s11242-007-9165-9

Laboratory and Simulation Investigation of Enhanced Coalbed Methane Recovery by Gas Injection

Kristian Jessen · Guo-Qing Tang · Anthony R. Kovscek

Received: 21 November 2006 / Accepted: 9 September 2007 / Published online: 12 October 2007

Abstract Methane/carbon dioxide/nitrogen flow and adsorption behavior within coal is investigated simultaneously from a laboratory and simulation perspective. The samples are from a coalbed in the Powder River Basin, WY. They are characterized by methane, carbon dioxide, and nitrogen sorption isotherms, as well as porosity and permeability measurements. This coal adsorbs almost three times as much carbon dioxide as methane and exhibits significant hysteresis among pure-component adsorption and desorption isotherms that are characterized as Langmuir-like. Displacement experiments were conducted with pure nitrogen, pure carbon dioxide, and various mixtures. Recovery factors are greater than 94% of the OGIP. Most interestingly, the coal exhibited ability to separate nitrogen from carbon dioxide due to the preferential strong adsorption of carbon dioxide. Injection of a mixture rich in carbon dioxide gives slower initial recovery, increases breakthrough time, and decreases the volume of gas needed to sweep out the coalbed. Injection gas rich in nitrogen leads to relatively fast recovery of methane, earlier breakthrough, and a significant fraction of nitrogen in the produced gas at short times. A one-dimensional, two-phase (gas and solid) model was employed to rationalize and explain the experimental data and trends. Reproduction of binary behavior is characterized as excellent, whereas the dynamics of ternary systems are predicted with less accuracy. For these coals, the most sensitive simulation input were the multicomponent adsorption–desorption isotherms, including scanning loops. Additionally, the coal exhibited a two-porosity matrix that was incorporated numerically.

Keywords CO_2 sequestration · Enhanced coalbed methane recovery · Multicomponent sorption · Hysteresis · Displacement experiments · Numerical simulation

K. Jessen (✉)
Chemical Engineering and Materials Science, University of Southern California, Los Angeles, CA 90089-1211, USA
e-mail: jessen@usc.edu

G.-Q. Tang · A. R. Kovscek
Energy Resources Engineering, Stanford University, Stanford, CA 94305-2220, USA

Nomenclature

a	Adsorbed concentration of a component
b	Co-volume of a component in the Peng Robinson EOS
B	Langmuir constant
C	Molar concentration of component in gas phase
L	Characteristic length
PV	Pore volume
PVI	Pore volumes injected
q	Volumetric flow rate
Q	Source/sink term for mass balance
t	Time
v	Total flow velocity
V	Volume
V_m	Langmuir constant
y	Mole fraction of a component in the gas phase
z	Mole fraction of a component in the adsorbed phase
α	Extended Langmuir isotherm parameter
β	Extended Langmuir isotherm parameter
ε	Coefficient used in numerical solution
ϕ	Porosity
ρ	Density
τ	Dimensionless time
ξ	Dimensionless distance
θ	Adsorbed amount of a component

Unit conversion

10^6 Pa(MPa)	145.04 pounds per square inch absolute (psia)
Kelvin (K)	to Farenheit (F): T(F)= (T(K) $\times$ 9/5) $-$ 459.67
Standard cubic feet per ton (SCF/ton)	$1.1953 * 10^{-3}$ moles/kg
10^{-3} Darcy (mD)	$0.9869 * 10^{-15}$ m^2

1 Introduction

Coalbed methane has grown in importance as an energy source in recent years and now accounts for about 10% of U.S. natural gas production. Coalbeds have large internal surface area and strong affinity for gases such as methane (CH_4) and carbon dioxide (CO_2). Gas is present both as a bulk phase in the pore space and on the solid in an adsorbed state at liquid-like density.

Effective methods to release fully the methane from tight coalbed resources have, yet, to be developed. Coalbed methane exploitation occurs, typically, through primary recovery using cavity-completed wells (Palmer et al. 1993). This completion technique is akin to hydraulic fracturing (Colmenares 2004). The coalbed is then dewatered to reduce pressure, so that methane desorbs from coal surfaces. Dewatering generally involves the pumping of significant quantities of water to the surface for disposal. Unfortunately, such primary methods typically recover less than half of the methane in a coalbed (Stevens et al. 1998). Injection of nitrogen (N_2) and CO_2, so-called enhanced coalbed methane recovery (ECBM),

is a means to increase the ultimate recovery. Field test results are reported elsewhere (Reeves 2001; Mavor et al. 2004).

Gas injection serves, firstly to maintain overall coalbed pressure and perhaps reduce the overall volume of water that must be lifted to the surface. Second, injecting a second gas, or a mixture of gases, serves to reduce the partial pressure of CH_4 in the free gas and thereby enhance desorption from coal surfaces. Gas injectants also sweep desorbed CH_4 through the reservoir.

Nitrogen is a natural choice for ECBM due to its availability and the fact that it tends to yield incremental recovery response relatively rapidly (Zhu et al. 2003). Carbon dioxide injection also has advantages in that CO_2 tends to adsorb to coal surfaces more strongly than either CH_4 or N_2 (adsorption results follow). The strong adsorption characteristics of CO_2 tend to impede premature breakthrough of injectant and result in more rapid complete displacement of CH_4 (Zhu et al. 2003). Carbon dioxide injection is also of interest due to the added benefit of CO_2 sequestration within coal. Moreover, CH_4 emits about half as much CO_2 when combusted, as compared to coal; there is synergy among ECBM and carbon sequestration.

Whereas equilibrium gas adsorption on coals is relatively well studied because the topic is related to mine safety (Joubert et al. 1974), the process model for ECBM and its numerical representation is not elucidated. Our previous analytical study of the flow of multicomponent gases through coal (Zhu et al. 2003) predicted an interesting interplay between the adsorption properties of coal surfaces and the advance of individual gas species. For instance, injection of pure CO_2 into a linear coal system leads to virtually 100% production of the original CH_4 in place prior to the breakthrough of CO_2. Injection of mixtures of N_2 and CO_2 into a CH_4 filled coal are predicted to be separated by the coalbed as CO_2 adsorbs more strongly to coal surfaces and is preferentially retained by the coalbed. Additional modeling attempts of note are well summarized in a recent review (Wei et al. 2005) that finds a general lack of understanding of the physical mechanisms occurring as CO_2 is injected into coal seams.

This lack of understanding motivated us to undertake a simultaneous experimental and numerical model validation study that builds upon our previous analytical modeling effort (Zhu et al. 2003). Our ultimate goal is to generate a suite of laboratory data that probes the transport of multicomponent, adsorbing gas mixtures through coal as well as sorption induced permeability changes of coal. This data suite is then useful for validation and ground truth exercises related to our modeling effort.

This article presents exploration of the unsteady flow of gas mixtures through one-dimensional coal systems. We also report new adsorption isotherms for a coal sample. The status of our companion investigations of coal permeability and the effect of moisture on gas adsorption and transport are summarized elsewhere (Harris et al. 2005). In the following sections, we describe our adsorption and flow apparatus and our formulation of an ECBM model. Characterization of the coal sample employed is then presented as are the experimental and numerical results for pure and mixed gas flow through coal. A discussion and conclusions complete the article.

2 Experimental Apparatus and Procedures

Experimental apparatus were constructed to measure equilibrium adsorption properties of coal samples as well as the transport of gaseous components through coal. All measurements

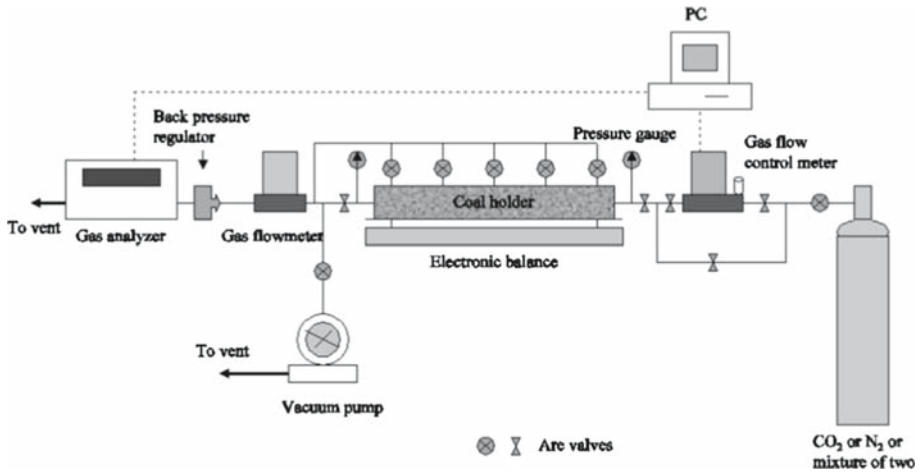

Fig. 1 Schematic of experimental apparatus for sorption, permeability, and displacement experiments

Table 1 Coalpack data, crushed Powder River Basin sample

Size of coal particles, cm	0.025
Pack length, cm	25.0
Diameter, cm	4.25
Total porosity, %	37
Permeability (helium), mD	31
Weight of coal, kg	0.231

were conducted using a single sample of coal from the Powder River Basin, WY. The coal originates from a coalbed at a depth of 274–366 m (900–1200 ft) below ground surface. Average in-situ pressure (Colmenares 2004) and temperature (Moore 2003) are estimated between 2480 and 3450 kPa (360–500 psia) and 301.15 and 305.15 K (82.4–89.6 F). The coal sample as received was not preserved at formation conditions, was extensively fractured and broken into small pieces, filled with formation water, and contained some clay or shale. The small size of intact pieces precluded the use of core samples. The large shale pieces were removed and the coal was ground to a particle size of about 60 mesh. This exposed the internal surface area of the coal. The ground samples were preserved in desiccators under vacuum to avoid surface oxidation. The mean size of the coal particles was 0.25 mm. The ground coal material was relatively easy to use. Coal particles were formed into a coalpack by pressing the ground coal into cylindrical shapes.

Figure 1 is a composite diagram of the experimental apparatuses. The centerpiece of these studies was the coalpack of 25 cm length and 4.25 cm diameter. Porosity and permeability of each pack were measured with helium (He) as reported in Table 1. It is assumed that helium did not adsorb to the coal surface. For adsorption and displacement studies, the coal was packed directly into an aluminum tube. This tube contained sampling ports along its length to provide measurements of flowing gas composition along the length of the apparatus.

At the inlet of the coalpack, either a pressure regulator, a gas-mass flow controller, or a constant volumetric gas flow device was used. The pressure drop across the coalpack was measured via pressure transducer to the nearest 0.7 kPa (0.1 psia). A back-pressure regulator at the coalpack outlet elevated the test pressure to the desired level. Downstream of the back-pressure regulator, a gas-flow rate meter measured the gas production rate at standard conditions. The effluent gas from the flow meter was then sent to a gas analyzer to measure the fraction of each gas species in the effluent mixture.

After completion of a flow experiment or a set of adsorption measurements, a vacuum pump was connected to the coalpack. The coalpack holder was placed on an electronic balance that measured the weight of the coalpack holder. Gas removal was verified by attainment of the original mass. The specific experimental procedures are described next.

2.1 Adsorption/Desorption Isotherms

All adsorption/desorption measurements were conducted at 295.15 K (71.6 F) using a gravimetric method. The coalpack was connected to the gas-supply cylinder (of known volume) directly through a pressure regulator. The outlet of the coalpack holder was closed. Except for the pressure transducer, all other components were removed to reduce dead volume. The coalpack was subjected to gas from the cylinder until the test pressure stabilized. When the weight of the coalpack was constant, it was recorded. The data was processed to obtain a total adsorption isotherm that accounts for the volume of the adsorbed phase (Mavor et al. 1990, and Clarkson and Bustin 2000). In short, the weight of free gas in the coalpack (W_f) was first estimated from the total pore volume, pressure, and gas compressibility. Second, the weight of adsorbed gas (W_a) was estimated from the total weight at equilibrium state (W_t) minus the weight of free gas. Next, the volume of adsorbed gas was computed from W_a and W_f was recomputed. After completion of iteration, the total adsorbed gas volume was then converted into gas volume at standard conditions.

The coalpack holder was then subjected to a greater/lesser pressure to obtain an adsorption/desorption isotherm. Adsorption continued until a maximum apparatus pressure was attained or in the case of CO_2, the pressure approached was critical. For desorption, the process was reversed and the pressure in the coalpack was gradually released. A minimum of 24 h was allowed following the stabilization of weight before the establishment of a new equilibrium pressure.

2.2 Gas Displacement

Displacement of coalbed methane was conducted under a variety of conditions. The coalpack was always vacuum evacuated first and then saturated with pure methane at test pressure. Note that experiments reported here are conducted under dry conditions.

Displacement tests were conducted at 2.90 MPa and 4.14 MPa (420 and 600 psia). The former pressure is representative of hydrostatic coalbed pressure, whereas the latter is, perhaps, representative of an elevated injection pressure that is less than the fracture pressure. The lower pressure tests were a part of our characterization procedures, such as the effect of injection rate on displacement effectiveness. Five displacement tests were conducted at 4.14 MPa (600 psia) with the following injectant compositions: 100% N_2, 100% CO_2, 85/15 % CO_2/N_2, 46/54% CO_2/N_2, 24/76% CO_2/N_2, respectively. The binary injection gas (CO_2/N_2) was prepared in a high-pressure cylinder equipped with a piston. Pure nitrogen was first injected

Table 2 Pure component parameters for the Langmuir isotherms reported in Figs. 2 and 3

	Adsorption		Desorption	
	V_m (SCF/ton)	B (1/psia)	V_m (SCF/ton)	B (1/psia)
CH_4	811	0.00237	543	0.0382
CH_4	scanning loop 2		498	0.0118
CH_4	scanning loop 3		510	0.0186
CO_2	1760	0.00521	1560	0.0158
N_2	272	0.00242	226	0.00574

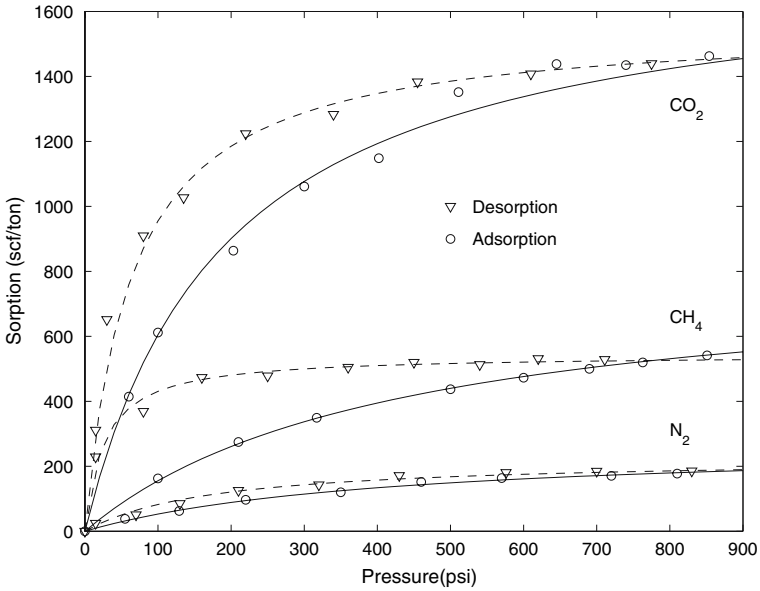

Fig. 2 Sorption characteristics of Power River Basin (Wyoming) coal. Measurements conducted at 295.15 K (71.6 F)

into the cylinder at a given pressure and thus the total moles are known. Then carbon dioxide was injected into the cylinder. After the mixing process is completed, the composition of the mixture is checked using the gas analyzer.

A flow experiment was initiated by beginning the acquisition of data from the pressure and gas analyzer systems. For tests at 2.90 MPa (420 psia), the gas flow controller was set to control mass flow rate. For tests at 4.14 MPa (600 psia), a high-pressure syringe pump injected water into one side of the piston/cylinder assembly thereby advancing the piston. Thus, gas was displaced at constant volumetric rate at system pressure. The nominal gas injection rate was 0.5 cm^3/min at test pressure. Pressure and composition were measured at 5 s intervals throughout the test.

3 Coal Characterization

Coalpacks were initially characterized by porosity and permeability measurements as given in Table 1. Pure component adsorption/desorption isotherms were measured (Table 2, Figs. 2 and 3). Then, pure CO_2 was injected to displace CH_4, at various pressures, to characterize the frontal advance of CO_2 in the coalbed (Figs. 4 and 5). These displacement experiments were performed to frame the subsequent numerical modeling work. Finally, the sensitivity of permeability to different gas species was investigated (Fig. 6). In the following subsections, we discuss the individual efforts towards coal characterization in more detail.

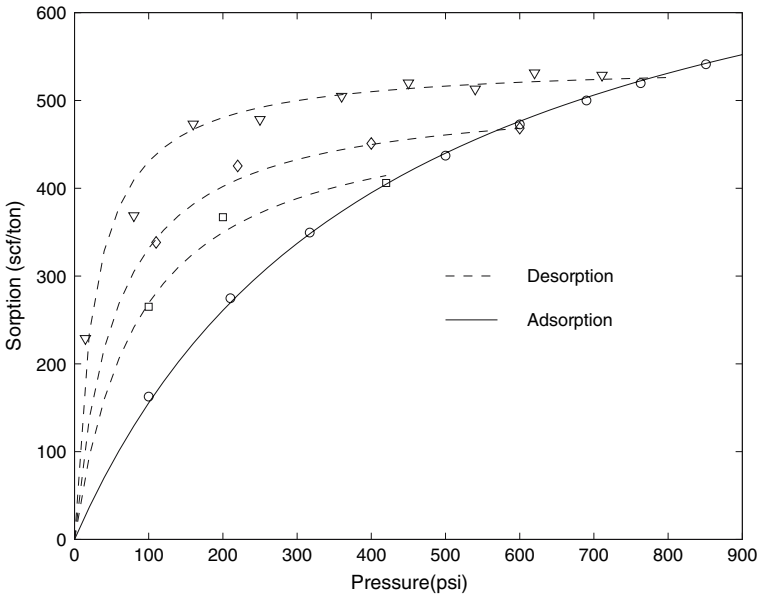

Fig. 3 Scanning loops for adsorption and desorption of CH_4 from Powder River Basin coal. Desorption curves depend on the initial pressure where depressurization begins. Measurements conducted at 295.15 K (71.6 F)

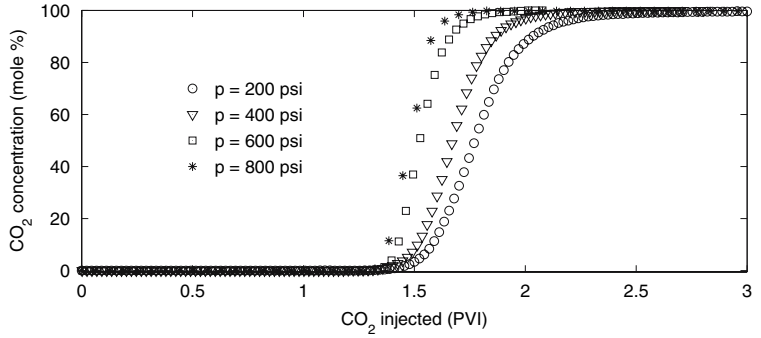

Fig. 4 Effect of pressure on CO_2 elution from coalpack. Injection rate is 0.5 cm^3/min at test pressure

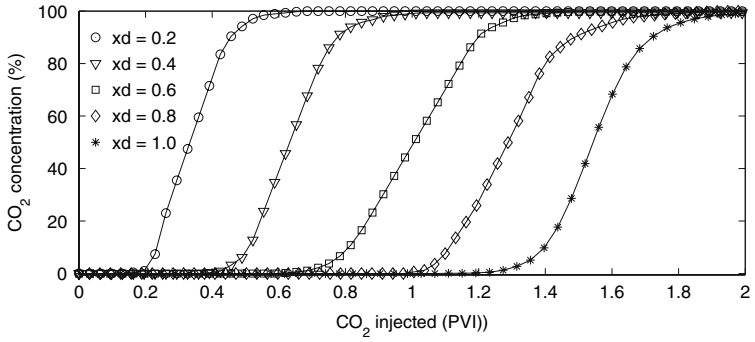

Fig. 5 CO_2 concentration versus time as sampled from various locations along the length of the coal pack. System backpressure maintained at 2.90 MPa (420 psia)

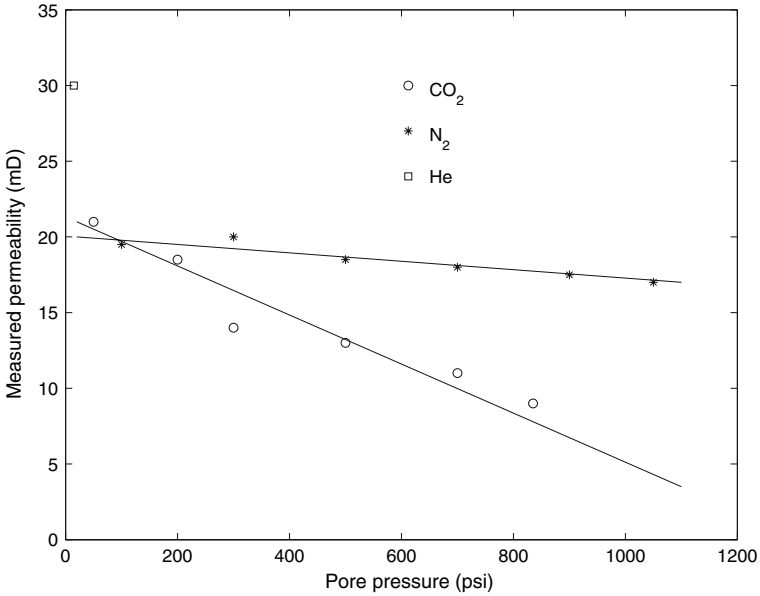

Fig. 6 Coalpack permeability versus pressure

3.1 Adsorption/Desorption Isotherms

Figure 2 presents the experimental observations of adsorption and desorption versus pressure for pure CH_4, CO_2, and N_2 at zero initial water saturation. Circles represent adsorption whereas triangles are for desorption. The curves shown in Fig. 2 are the best-fit using the Langmuir-isotherm

$$\theta = \frac{V_m \cdot B \cdot p}{1 + B \cdot p} \tag{1}$$

where θ is the adsorbed amount per mass of coal, p is the pressure and V_m, B are the Langmuir parameters. The Langmuir parameters (V_m, B) corresponding to the curves presented in Fig. 2

are reported in Table 2. It appears adequate for description of pure gas adsorption/desorption behavior. For methane, the maximum adsorption is roughly 550 scf/ton (0.66 mole/kg), at 6.5 MPa (950 psia). From the slope of the adsorption data, it appears that further methane adsorbs on the surface at greater pressure. There is significant hysteresis between adsorption and desorption curves. During desorption there is little response to pressure decline from 6.90 to 1.03 MPa (1000–150 psia). The majority of methane desorbs at pressures below 1 MPa (145 psia). Thus, methane production from such coal bed reservoirs by a depletion process must reach low pressures to release methane from coal surfaces.

Carbon dioxide adsorption/desorption curves versus pressure also display significant hysteresis and follow a Langmuir-type relationship. Whereas hysteresis may be detrimental to methane recovery during primary depletion, it has benefit during CO_2 sequestration. Hysteretic CO_2 loading and unloading in Fig. 2 indicates that coal surfaces retain significant volumes of CO_2 even though they may experience pressure reduction. Moreover, carbon dioxide adsorption is significantly greater than methane at the same pressure. The maximum carbon dioxide adsorption is about 1450 scf/ton (1.73 mole/kg) at the pressure of 5.79 MPa (840 psia). That is, roughly 3 times the loading of methane at that pressure. Note that the critical pressure for carbon dioxide is about 7.38 MPa (1070 psia). Our apparatus is not currently configured for supercritical CO_2.

The nitrogen adsorption/desorption behavior displays characteristics similar to CH_4 and CO_2. Its adsorption capacity is the least among the three test gases. Nitrogen desorption shows less hysteresis, in an absolute sense, than that observed for carbon dioxide and methane. Comparison of nitrogen and carbon dioxide curves teaches that the coal surface holds nearly 6 times the volume of carbon dioxide relative to nitrogen. For strictly enhancing coal bed methane recovery, nitrogen injection may be favored owing to smaller loss of the injectant to the coal surface.

The adsorption hysteresis displayed by all gases raises several interesting questions. One question is the dependence of the desorption characteristics on the initial pressure of the coal sample. Figure 3 illustrates that for methane, the desorption isotherm followed during pressure reduction is a function of the maximum pressure achieved during adsorption. The desorption path followed differs as the initial maximum gas pressure decreases from 6.55 to 4.14 to 2.76 MPa (950 to 600 to 400 psia) This is similar to so-called scanning loops measured for capillary pressure as a function of water saturation for rocks and soils. Carbon dioxide and N_2 likely display similar scanning loops. This dependence of desorption path on initial pressure is still to be investigated thoroughly.

Some authors (Clarkson and Bustin 2000) state that hysteresis in adsorption and desorption curves is attributable to experimental errors. The most often cited error is a change in the moisture content of the coal. Our samples are, however, dry as are the injectants. Moreover as illustrated in Fig. 3, it is possible to attain repeatable adsorption values, during reloading of the surface, that fall on the original adsorption curve when cycling from adsorption to desorption and back to adsorption. Surface geometry heterogeneity likely accounts for adsorption/desorption hysteresis as found here (Seri-Levy and Avnir 1993). Seri-Levy and Avnir used Monte Carlo simulations of gas–solid systems are to examine gas adsorption on rough surfaces of various geometries. They computed significant hysteresis in equilibrium isotherms as a result of path dependent configurations of adsorbed molecules. Additionally, they changed the degree of hysteresis by changing the surface structure.

3.2 Carbon Dioxide Displacement

An initial set of gas displacements were conducted to characterize the nature of CO_2 movement in the coalpacks. In the first set of experiments, pure CO_2 was injected at a variety of pressures. The CO_2 was compressed to a pressure equal to pore pressure in the piston-cylinder pressure vessel. Tests were conducted at pressures ranging from 1.38 to 5.52 MPa (200 to 800 psia). The gas composition and outflow rate were measured versus time. Figure 4 shows the produced CO_2 concentration profile versus injected volume at the four different pressures. The CO_2 breakthrough time was similar for all cases; however, after breakthrough, effluent CO_2 concentration behaved somewhat differently. At high pressure, the effluent concentration increases sharply, indicating that the displacement is piston-like. When the pressure is lower, the effluent CO_2 concentration is more dispersed. The observed behavior is consistent with the idea that the adsorption rate is a function of gas partial pressure and greater pressure shortens the time for CO_2 to replace CH_4 from coal surfaces. Nevertheless, any dynamics for gas exchange appear to be fast relative to the rate of gas movement through the coal.

The sampling ports along the length of the coal pack allow measurement of the composition of the free gas during tests. Figure 5 displays a typical result for gas composition measured at fractions of 0.2, 0.4, 0.6, 0.8, and 1 of the total length of the core. In this experiment, the pressure was 2.90 MPa (420 psia). The injection rate was 0.5 cm^3/min at test pressure. Upon reaching a sampling port along the core, the concentration of CO_2 in the free gas increased rapidly and smoothly to the injection composition of 100%. The CO_2 concentration profiles within the coal pack evolved quickly to become nearly piston like, and indicate that CH_4 was displaced effectively by CO_2.

3.3 Coalpack Permeability

Steady-state coalpack permeability was measured for helium, N_2, and CO_2 as a function of pore pressure, Fig. 6. In all cases, measurements are made after at least 8 PVI. This allows sufficient time for the coal to equilibrate with gas. Values are accurate to roughly 0.2–0.3 mD. The permeability to helium at low pressure is about 30 mD. Clearly, the coalpack permeability is sensitive to the gas species. Note that the permeability to N_2 is about 20 mD at low pressure. Also note that from 0.69 MPa to 5.52 MPa (100 to 800 psia) the permeability to N_2 is roughly constant. On the other hand, coalpack permeability is substantially more sensitive to CO_2 pressure. Between 0.69 and 4.14 MPa (100 and 600 psia), permeability decreases by almost 50%, from 20 to roughly 12 mD.

In summary, initial results indicate: (i) one-dimensional flow is achievable in these coalpacks, (ii) frontal advance is sufficiently rapid that diffusion and dispersion along the axial direction are negligible, (iii) gravity is negligible in such displacements, (iv) adsorbed gases occupy volume that must be incorporated when measuring total gas adsorption and (v) the Langmuir isotherm adequately models pure gas adsorption.

4 ECBM Model

Our starting points are the analytical model and concomitant assumptions of Zhu et al (2003) They are consistent with the initial experimental results reported above. The governing equation for single-phase flow of gas species i in a porous medium including sorption is written

$$\phi \frac{\partial C_i}{\partial t} + (1-\phi)\frac{\partial a_i}{\partial t} + \nabla \cdot (\underline{v} C_i) = q_i. \tag{2}$$

The symbol C_i is the molar concentration of component i in the gas phase

$$C_i = y_i \rho_y, \tag{3}$$

where y_i is the mole fraction of component i in the gas phase and ρ_y is the molar density of the gas phase. Next, a_i is the molar concentration of component i adsorbed on the coal surface. The adsorbed amount is obtained from the extended Langmuir isotherm (Markham and Benton 1931) that employs only pure component isotherm parameters

$$a_i = \frac{\alpha_i \beta_i y_i}{1 + \sum_k \beta_k y_k} \tag{4}$$

where

$$\alpha_i = \rho_{i,\mathrm{std}} \rho_{\mathrm{coal}} V_{m,i}. \tag{5a}$$

$$\beta_i = B_i p \tag{5b}$$

In Eq. 5, $\rho_{i,\mathrm{std}}$ is the molar density of pure component i at standard conditions (101.325 kPa, 288.15 K), ρ_{coal} is the mass density of the (solid) coal sample, $V_{m,i}$ and B_i are Langmuir constants for a pure gas species and p is the displacement pressure. In the third term on the left of Eq. 2, the overall flow velocity is denoted v.

Additionally, the ground coal particles have internal porosity. A typical matrix porosity for coal is 2–8% (Resnik et al. 1984; Mavor et al. 1999) and this porosity is exhibited within coal grains. We term the grain porosity secondary porosity, ϕ_2. Secondary porosity is dead-end pore space that does not contribute to the overall flow, but participates in the adsorption of gases. The secondary porosity is assumed to be in instantaneous equilibrium with the bulk phase composition of the primary pore porosity (ϕ_1). Accordingly, the overall porosity of the coal packs are written

$$\phi = \phi_1 + \phi_2 \tag{6}$$

We do not have direct measurements of the secondary porosity of our coal packs. Secondary porosity is implemented as a single adjustable parameter to match the binary displacement experiments to follow.

Equation (2) is rewritten for one-dimensional (1D) flow, the primary/secondary porosity concept is implemented, and time and distance are nondimensionalized as τ and ξ respectively

$$\frac{\partial C_i}{\partial \tau} + \frac{(1-\phi)}{\phi} \frac{\partial a_i}{\partial \tau} + \frac{\partial v_d C_i}{\partial \xi} = Q_i, \tag{7}$$

with

$$\tau = \frac{v_{\mathrm{inj}} t}{\phi L} \tag{8a}$$

$$\xi = \frac{x}{L} \tag{8b}$$

$$v_d = \left(\frac{v}{v_{\mathrm{inj}}}\right)\left(\frac{\phi}{\phi_1}\right). \tag{8c}$$

4.1 Numerical approach

The conservation equations were solved numerically using explicit time stepping and single-point upstream weighting of component fluxes. The adsorption and desorption of gas molecules on the coal surface during the displacement of CH_4 introduces a sharpening behavior of the species concentration within the gas phase that renders the displacement calculations significantly less sensitive to numerical diffusion than traditional convection dominated flows. Hence, no requirement for more sophisticated numerical schemes was suggested to reduce artificial diffusion. Phase properties were predicted by the Peng-Robinson (PR) equation of state (EOS) (Peng and Robinson 1976). For the purpose of evaluating phase behavior, we assumed that the pressure drop along the displacement length was negligible and used the value of the initial pressure throughout the displacement calculation.

As gas is injected into the coal pack and partitions between the coal surface and the free gas phase, new mixtures are formed with partial molar volumes different from the original fluid in place. In addition, gas species adsorb with different affinity to the coal surface, as seen from the sorption measurements. Thus, the porosity is partially filled with immobile adsorbed species. Computationally, the secondary porosity is filled before filling the primary porosity. Accordingly, volume change of the adsorbed species on mixing/sorption plays a role and was included in the simulation of the displacement processes.

We approximated the volume occupied by the adsorbed phase (V_{ads}) using

$$V_{\text{ads}} = \sum\nolimits_i z_i b_i \tag{9}$$

as recommended by Hall et al. (1990), where b_i is the hard-sphere, co-volume of component i predicted by the PR EOS and z_i is the mole fraction of component i in the adsorbate ($z_i = a_i / \sum a_k$). This is, in fact, identical to the procedure used to obtain volume of the adsorbed phase during adsorption/desorption measurements.

As the pressure equation (volume balance) is not solved at each time step during the simulation, an explicit correction of the local flow velocity is applied to ensure simultaneous volume and mass conservation. In the explicit treatment, we carry any volume discrepancy forward in time and correct the velocities of a grid cell k by (Gerritsen et al. 2005)

$$v_{d,k+1/2} = v_{d,k-1/2} + \varepsilon \frac{\Delta\tau}{\Delta t}(q_{vc} - 1), \tag{10}$$

where $q_{vc} = V_{\text{fluid}} / V_{\text{cell}}$ and the coefficient $\varepsilon (< 1)$ is introduced to ensure stability of the overall numerical scheme.

5 Gas Flow in Coalbeds

First results for binary gas flow are presented followed by ternary results.

5.1 Binary Displacements

The measured sorption isotherms, permeability, and porosity were used as input for calculation of the displacement of pure CH_4 by pure CO_2 and pure CH_4 by pure N_2 at 4.14 MPa (600 psia). The secondary porosity is unknown. It was adjusted such that simulated breakthrough times matched experimental observations for the binary displacements. The value of ϕ_1 obtained was 7.4% relative to the overall porosity of 37%. This value of the secondary

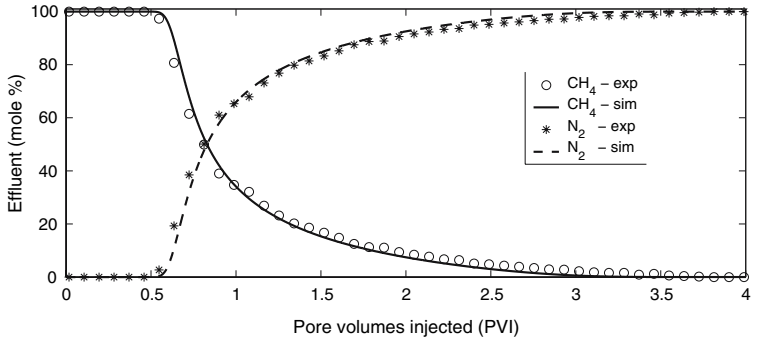

Fig. 7 Experimental (symbols) and simulated (lines) production for pure N_2 displacing CH_4 at 4.14 MPa (600 psia)

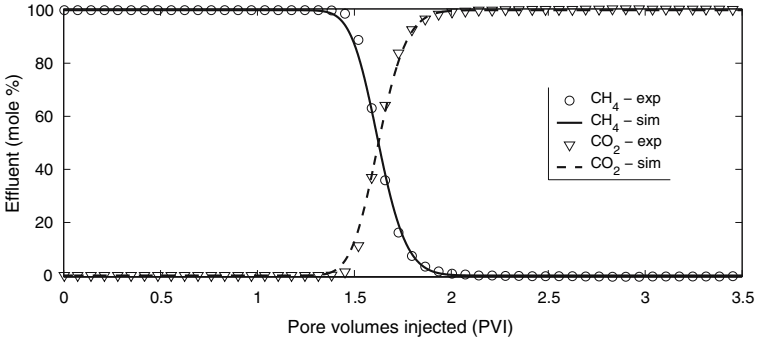

Fig. 8 Experimental (symbols) and simulated (lines) production for pure CO_2 displacing CH_4 at 4.14 MPa (600 psia)

porosity is in excellent agreement with coal matrix porosities reported elsewhere (Resnik et al. 1984; Mavor et al. 1999).

Figures 7 and 8 present the production profiles resulting from the injection of CO_2 and N_2. That is, the concentration at the outlet versus the pore volume of gas injected (PVI) is presented. The gas flood results from experiment and simulation are in substantial agreement. The different injection gases yield different production response as detailed next.

Nitrogen injection presented in Fig. 7 yields injectant breakthrough at the outlet in about 0.55 PVI. Thereafter, both nitrogen and methane are produced, with decreasing CH_4 concentration, until 2.9 PVI. For injection volumes greater than 1 PVI, CH_4 concentration in the effluent gas gradually tails to zero. More than 3 PVI of N_2 were injected to displace movable CH_4. This behavior indicates that CH_4 recovery by injecting N_2 is a slow process with significant mixing of the injected gas and original gas in place.

Figure 8 presents the results for pure CO_2 injection. CO_2 breaks through to the outlet about 1 PVI later than N_2 at 1.5 PVI. At breakthrough, 20.0 g of CO_2 has been injected. Excluding the free CO_2 in pore spaces, the amount of adsorbed CO_2 is nearly equal to its equilibrium adsorption, verifying that the displacement of CH_4 by pure CO_2 is nearly piston-like. Methane concentration in the effluent gases reaches zero by 2 PVI.

5.2 Ternary Displacements

With the exception of the composition of the injection gas, parameters and boundary conditions identical to the binary displacement simulations were used to predict the results of ternary displacements. That is, no parameter adjustment occurred. Figures 9 to 11 present

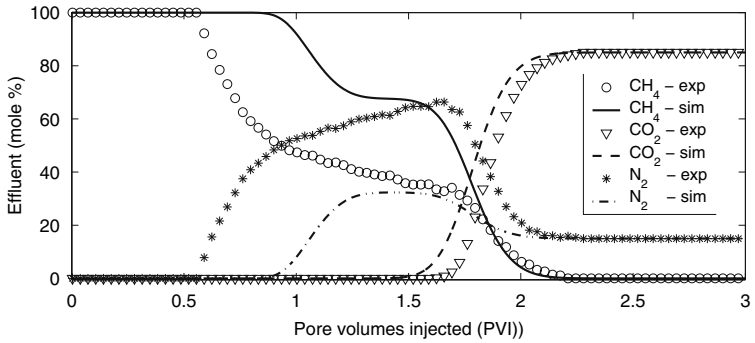

Fig. 9 Experimental (symbols) and simulated (lines) production for 85/15 CO_2/N_2 mixture displacing CH_4 at 4.14 MPa (600 psia)

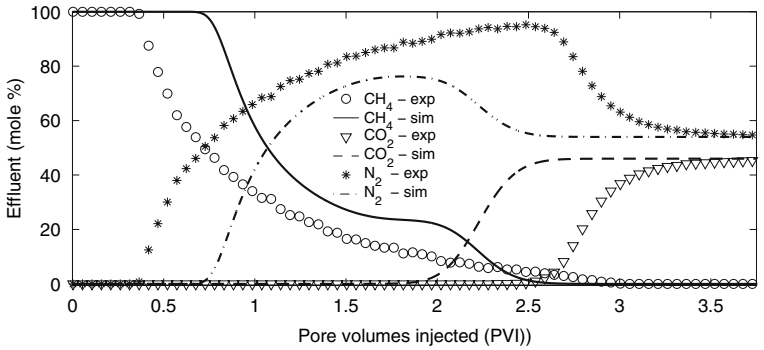

Fig. 10 Experimental (symbols) and simulated (lines) production for 46/54 CO_2/N_2 mixture displacing CH_4 at 4.14 MPa (600 psia)

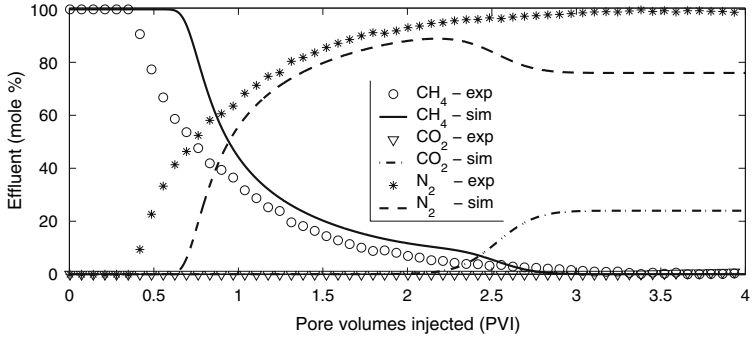

Fig. 11 Experimental (symbols) and simulated (lines) production for 24/76 CO_2/N_2 mixture displacing CH_4 at 4.14 MPa (600 psia)

the comparisons among experimental and simulation results. Qualitatively, similar trends are observed as the fraction of CO_2 in the injection gas decreases from 85 to 46 to 24%; however, the agreement is far from exact. The discussion presents some possible explanations for these discrepancies.

Figure 9 gives the effluent gas concentration versus injected gas volume for CH_4 displacement by a mixture of 85/15 CO_2/N_2. The N_2 breaks through to the outlet at 0.55 PVI. This time is nearly identical to the pure N_2 result. Similar to the pure N_2 injection, N_2 serves primarily as a displacing agent to drive methane from the pore spaces. After N_2 breakthrough, its concentration increases quickly and is even briefly greater than the injected concentration. Elevated N_2 concentration occurs because the injected CO_2 is adsorbed by the coal surfaces and the volume of methane released is less than adsorbed CO_2. Note that adsorption of carbon dioxide at a partial pressure of 3.52 MPa (510 psia = 0.85·600) is about 2.5 times that for pure CH_4 at 4.14 MPa (600 psia). Thus, the concentration of N_2 in the produced gas is elevated. The experimentally measured concentrations are greater, however, both experiment and simulation display clear banking of N_2.

The greatest nitrogen concentration in the experimental effluent gases is about 66% at 1.7 PVI. Thereafter, the produced N_2 concentration decreases to the injected concentration of 15% by roughly 2 PVI. Carbon dioxide breaks through to the outlet between 1.5 and 1.7 PVI. Carbon dioxide concentration in the effluent gases then increases sharply to the injected value of 85% indicating piston-like advance. Methane production terminates somewhat later at 2.2 PVI in comparison to pure CO_2 injection.

Carbon dioxide concentration in the injected gas was next decreased to 46%, Fig. 10. Experimentally, N_2 breaks through at 0.4 PVI which is about 0.1 PVI earlier than that for injection of a pure N_2 or the 85/15 CO_2/N_2 mixture. The CO_2 break through is in excess of 2 PVI for both experiment and simulation. The concentration of CO_2 in the effluent increases quickly, in both cases, from 0 to 46% consistent with significant CO_2 retention and pistonlike advance. By 2.5 PVI, methane production is essentially complete, although the experiments do exhibit some tailing out.

Next consider results for injection of 24/76 CO_2/N_2, Fig. 11. Nitrogen in the experiment breaks through at 0.4 PVI, similar to the previous case. The simulated breakthrough time of N_2 is about 0.6 PVI. Carbon dioxide, however, breaks through at greater than 2 PVI in both experiment and simulation; however, breakthrough times are not in agreement. Simultaneously, the CH_4 concentration in effluent gases decreases with time and reaches zero at roughly 3 PVI.

Consistent with results from injection of the previous two gas mixtures, the coal surfaces affect a chromatographic separation of N_2 and CO_2. In simple terms, CO_2/N_2 injection gases embody two mechanisms. The CO_2 functions mainly to displace methane from coal surfaces, whereas N_2 serves as a displacing agent to drive CH_4 from the coalpack. For all mixtures and consistent among experiment and theory, the breakthrough of CO_2 signals that the end of CH_4 production is imminent.

6 Summary and Discussion

Figure 12 presents a summary of the recovery of original CH_4 in place versus PVI. It also compares experiment, Fig. 12 (top), and simulation, Fig. 12 (bottom). The measured, ultimate recovery of CH_4 is greater than 94% in all cases. Recovery is obtained from the measured effluent concentration of CH_4 and the flow rate at the coalpack exit. The measurement of effluent flow rate is subject to considerably more uncertainty than the concentration measu-

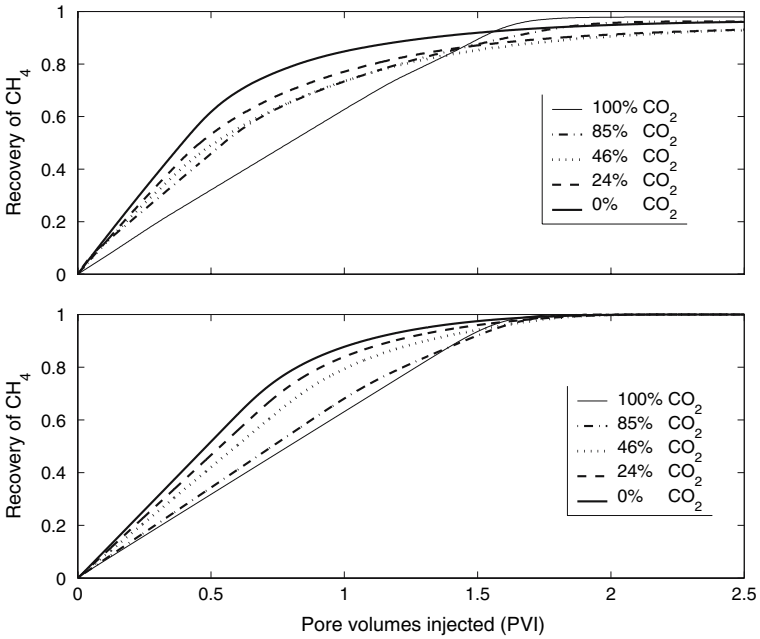

Fig. 12 Fraction of original CH_4 in place that is displaced: (top) experimental recovery and (bottom) simulated recovery

rement. The error in the reported recovery is estimated at 4% of the original gas in place. There is no residual gas or irreversible adsorption in the simulations and, hence, simulated recovery is 100%.

In both experiments and simulation, the initial recovery rate decreases as the fraction of CO_2 in the injection gas increases. Injection gases rich in CO_2 experience significant volume reduction because of significant uptake of CO_2 by the coal surface. Adsorption, thereby, reduces the flow velocity of the injection gas.

Comparison of Figs. 9 to 11 and 12 teaches that in ternary displacements we overpredict the rate of CH_4 recovery as well as the concentration of CH_4 in the effluent gas. The experimental observations for the ternary displacements show a consistently earlier breakthrough of N_2 and a later breakthrough of CO_2 relative to the numerical calculations. Three are possible explanations for the discrepancies between the experimental observations and the simulated behavior of the ternary displacements are: (i) mass transfer limitations for gas exchange, (ii) geomechanical effects resulting from coal shrinkage and swelling with gas loading, and (iii) prediction of multicomponent sorption behavior.

We do not believe that significant mass transfer resistance is exhibited in our experiments. This assertion is supported by the binary displacement results that present almost exact agreement between experiment and theory without incorporation of rate effects, Figs. 7 and 8. Secondly, the coal particles are 0.25 mm in diameter and, correspondingly, the times for diffusive exchange of gas species from the particle exterior to the center of the particle are quite short. Crank (1958) solves the unsteady diffusion equation in spherical coordinates under the conditions of a uniform initial concentration and a constant concentration at the sphere boundary. Refer to his Fig. 6.1 and Eqs. 6.18–6.20. For diffusivities from 10^{-7} to 10^{-5} m^2/s, the time required for the concentration of a gas species at the center of the

spherical grain to increase from 0 to 95% of the concentration of gas on the exterior of the sphere ranges from 0.1 to 10^{-4} s, respectively. The time needed for gas to diffuse across a stagnant boundary layer on the particle surface is similarly short.

With respect to geomechanical effects, the discrepancy among experimental and simulation results for ternary systems does exhibit behavior that at first glance is interpretable as arising from shrinkage and swelling of coal particles. Nitrogen consistently breaks through during experiments more quickly than predicted. This is perhaps consistent with shrinkage and increase in permeability of the N_2 occupied sections of the coalpack. Similarly, the experimental breakthrough of CO_2 later than predicted appears to be consistent with swelling and permeability reduction. Nevertheless, the exact match of binary displacement behavior for N_2/CH_4 and CO_2/CH_4 with identical values of coalpack permeability and no evolution of permeability as CO_2 permeates the pack obviates the argument that swelling is important to the results of these laboratory, ternary displacements. Lastly, the reader is reminded that we did characterize shrinking/swelling behavior as it relates to permeability of these coalpacks, Fig. 6. Nitrogen flows across the spectrum of pressure from 0.69 to 5.52 MPa (100 to 800 psia) with no change in permeability of the coalpack. Shrinkage does not appear to be responsible for the more rapid breakthrough of N_2 than expected in ternary systems.

The representation of multicomponent sorption phenomena, including scanning loops and hysteresis, is the most likely source of discrepancy. Initial prediction of the binary cases employing the extended Langmuir equation suggested that it approximated sorption adequately for estimation of flow results. The extended Langmuir equation predicts a constant selectivity for CO_2 adsorption over CH_4, and similarly a constant selectivity for N_2 is suggested. Some adsorption studies state that such selectivity is a function of total gas pressure and gas species concentration (Clarkson and Bustin 2000). For instance, the selectivity of N_2 for the coal surfaces in our study increases as the total gas pressure increases (Lin et al. 2007). The dynamics of gas transport in our study are clearly affected by the details of gas adsorption. The effluent data observed for the ternary displacements suggest that the mass of N_2 adsorbed on the coal surface, relative to that predicted by the extended Langmuir equation, decreases in the presence of CH_4 and CO_2 at a fixed pressure. Consequently, the predicted propagation velocity of N_2 through the coalpack is less than what is observed from the experiments. Similarly, the effluent data suggest that CO_2 selectivity is enhanced resulting in later actual breakthrough times in comparison to predictions.

In order to illustrate the sensitivity of flow prediction to the sorption model, an additional simulation was conducted for the 46/54 CO_2/N_2 injection gas. Figure 13 reports two cases. Case 1 was identical to the numerical result in Fig. 10. Case 2 was obtained using only the desorption isotherm for N_2 reported in Fig. 2. That is, there is no hysteresis in N_2 sorption in the calculation. The sorption behavior of pure CH_4 and CO_2 was unchanged and again the extended Langmuir equation is used to predict multicomponent adsorption. With changes to only the N_2 sorption characteristics, the breakthrough time for CO_2 has been reduced about 0.3 PV and the elution curve for CH_4 gas changed dramatically. About 0.3 PVI less time is required to sweep out all of the CH_4. The breakthrough time for N_2 is virtually unchanged, but the area under the nitrogen elution curve has decreased somewhat.

Clearly, the representation of ternary and greater adsorption phenomena within the framework of gas adsorption, desorption, and transport is an area where we continue investigation. Moreover, gas adsorption on coal surfaces needs to be characterized more fully including scanning loops.

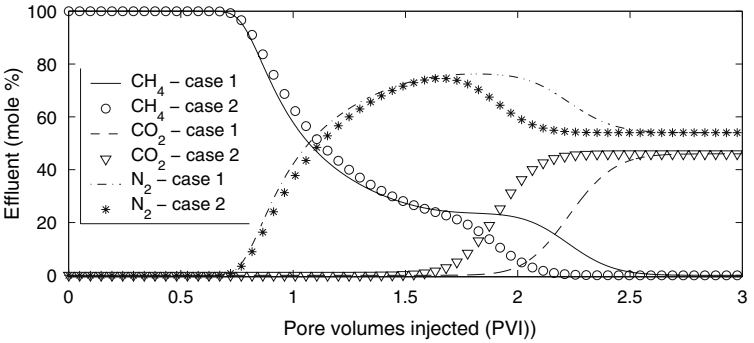

Fig. 13 Comparison of simulation results for a 46/54 CO_2/N_2 mixture displacing CH_4 at 4.14 MPa (600 psia). Case 1 is the result from Fig. 10. Case 2 employs slightly modified adsorption behavior for N_2 with no changes to CH_4 and CO_2

7 Conclusions

The interplay of gas sorption and transport in coal yields a rich dynamical behavior. Injection of mixtures with a large fraction of CO_2 reduces the initial recovery rate but increases breakthrough time as well as decreases the total amount of injectant needed to sweep out the coalbed. The experimental program verifies that coalbeds are useful to separate chromatographically N_2 and CO_2 while at the same time coalbed methane is recovered.

The simulations and experiments lead to the following specific conclusions:

1. Pure CH_4, CO_2, and N_2 adsorption on crushed Wyoming Powder River Basin coal is well represented by the Langmuir isotherm. The adsorption capacity of carbon dioxide is about 3 times greater than methane and 7 times greater than nitrogen.
2. Gas injection enhances CBM recovery significantly. Experimental recoveries of the original gas in place are in excess of 94% for all cases.
3. Experiment and simulation show consistently that carbon dioxide moves through coal in a piston-like fashion; thus, breakthrough times for CO_2 are significantly large. The least measured breakthrough time corresponded to 1.5 PVI.
4. Nitrogen advances more rapidly and displays a more dispersed front, in comparison to CO_2. Following breakthrough, significant mixing of injected N_2 and initial gas is measured at the production end in all cases.
5. The transient behavior of binary gas systems is well represented in a quantitative and qualitative sense by the numerical model. The qualitative behavior of ternary gas systems is well represented in simulation results; however, quantitative agreement of breakthrough times and the elution profiles for gas species remains to be proven.
6. Numerical representation of the dynamics of multicomponent gas transport through coal beds is quite sensitive to the representation of sorption phenomena. Such phenomena include hysteresis, scanning loops, and the selectivity of a gas species for coal surfaces as a function of pressure and free gas composition.

Acknowledgements We acknowledge gratefully the Global Climate and Energy Project of Stanford University and the financial support of its sponsors.

References

Clarkson, C.R., Bustin, R.M.: Binary gas adsorption/desorption isotherms: effect of moisture and coal composition upon carbon dioxide selectivity over methane. Int. J. Coal Geol. **42**, 241–271 (2000)

Colmenares, L.B.: Rock strength under true axial loading, seismotectonics of northern south america, and geomechanics and coal bed methane production in the Powder River basin, Ph.D. Thesis, Stanford University, Stanford, CA (2004)

Crank, J.: The Mathematics of Diffusion. pp. 85–87. Oxford University Press, Oxford, U.K. (1958)

Gerritsen, M.G., Jessen, K., Lambers, J.V., Mallison, B.T.: A fully adaptive streamline framework for the challenging simulation of gas-injection processes. Paper SPE 97270 presented at the SPE Annual Technical Conference and Exhibition, Dallas, TX 8–12 Oct. 2005

Harris, J., Kovscek, A.R., Orr, F.M. Jr., Zoback, M.D.: Geologic CO_2 sequestration, 2004–05 technical report of the global climate and energy project (GCEP), Stanford University, (2005) http://gcep.stanford.edu/research/technical_report.html

Hall, F.E., Zhou, C., Gasem, K.A.M., Robinson, R.L., Yee, D.: Adsorption of pure methane, nitrogen, and carbon dioxide, and their binary mixtures on wet fruitland coal. Paper SPE 29194 presented at the SPE Eastern Regional Conference and Exhibition, Charleston, WV, 23–26 Sept. 1990

Joubert, J.I., Grein, C.T., Bienstock, D.: Efffect of moisture on the methane capacity of american coals. Fuel, **53**(3) 186–191 (1974)

Lin, W., Tang, G.-Q., Kovscek, A.R.: Sorption-Induced Permeability Change of Coal During Gas Injection Process. Paper SPE 109855 presented at the SPE Annual Technical Conference and Exhibition, Anaheim, CA 11–14 Nov. 2007

Mavor, M.J., Gunter, W.D., Robinson, J.R.: Alberta mulitwell micro-pilot testing for CBM properties, enhanced methane recovery, and CO_2 storage potential. Paper SPE 90256 presented at the SPE Annual Technical Conference and Exhibition, Houston, TX 26-29 Sept. 2004

Markham, E.C., Benton, A.F.: The adsorption of gas mixtures by silica. J. Am. Chem. Soc **53**(2) 497–507 (1931)

Mavor, M.J., Owen, L.B., Pratt, T.J.: Measurement and evaluation of coal sorption isotherm data. Paper SPE 20728 presented at the SPE Annual Technical Conference and Exhibition, New Orleans, LA 23–26 Sept. 1990

Mavor, M., Pratt, T., DeBruyn, R.: Study quantifies powder river coal seam properties. Oil&Gas J., 35–41 (1999)

Moore, W.R.: Geothermal gradient of the Powder River Basin, Wyoming. Paper presented at the AAPG Annual Meeting, Salt Lake City, UT, U.S.A. 11–14 May, 2003

Palmer, I.D., Mavor, M.J., Spitler, J.L., Seidle, J.P., Volz, R.F.: Openhole cavity completions in coalbed methane wells in the San Juan basin. J. Petr. Tech. **45**(11) 1072–1080 (1993)

Peng, D.Y., Robinson, D.B.: A new two-constant equation of state. Ind Eng. Chem Fund. **15**, 59–64 (1976)

Reeves, S.R.: Geological sequestration of CO_2 in deep, unminable coalbeds: an integrated research and commercial-scale field demonstration project. Paper SPE 71749 presented at the SPE Annual Technical Conference and Exhibition, New Orleans, LA, 30 Sept. – 3 Oct. 2001

Reznik, A.A., Singh, P.K., Foley, W.K.: An analysis of the effect of CO_2 injection on the recovery of in-situ methane from bituminous coal: an experimental simulation. Soc. Pet. Eng. J. **24**(5) 521–528 (1984)

Seri-Levy, A., Avnir, D.: Effects of heterogeneous surface geometry on adsorption. Langmuir **9**, 3067–3076 (1993)

Stevens, S.H., Spector, D., Reimer, P.: Enhanced coalbed methane recovery using CO_2 injection: worldwide resource and CO_2 sequestration potential. Paper SPE 48881 presented at the 1998 SPE International Oil & Gas Conference and Exhibition in China, Beijing 2–6 November, 1998

Wei, X.R., Wang, G.X., Massarotto, P.: A review of recent advances in the numerical simulation for coalbed methane recovery process. Paper SPE 93101 presented at the Asia Pacific Oil & Gas Conference and Exhibition, Jakarta Indonesia, 5–7 Apr. 2005

Zhu, J., Jessen, K., Kovscek, A.R., Orr, F.M. Jr.: Analytical theory of coalbed methane recovery by gas injection. Soc. Pet. Eng. J. **8**(4) 371–379 (2003)